# Absolute Configuration Determination and Convenient Asymmetric Synthesis of *cis*-3-(9-Anthryl)cyclohexanol with Proline as a Catalyst

JĘDRZEJ WYSOCKI, MARCIN KWIT, AND JACEK GAWRONSKI*
*Department of Chemistry, Adam Mickiewicz University, Poznan, Poland*

*ABSTRACT* *cis*-(3*R*)-(9-anthryl) derivative of cyclohexanol was conveniently obtained in enantiomerically pure form from 2-cyclohexenone using asymmetric Michael addition of anthrone catalyzed by L-proline in a key step. The absolute configuration of the addition product was unequivocally determined by means of electronic circular dichroism measurements combined with calculation of the circular dichroism spectrum by using a density functional theory method. *Chirality 00:000–000, 2012.* © 2012 Wiley Periodicals, Inc.

*KEY WORDS:* asymmetric catalysis; proline; conjugate addition; circular dichroism; DFT calculations

## INTRODUCTION

Enantiomerically pure 3-substituted cyclohexanones and cyclohexanols are of considerable interest as model molecules for stereochemical studies. Compounds of this type are accessible most directly by conjugate addition of an appropriate nucleophile to 2-cyclohexenone (**1**). With a chiral catalyst, nonracemic addition product **3** can be obtained (Scheme 1).

Examples of such additions range from asymmetrically catalyzed additions of organometallic reagents[1–4] to additions of thiols[5,6] or 1,2,4-triazole;[7] the last two are catalyzed by Cinchona alkaloid derivatives. Anthrone (**2**) is an atypical nucleophile because its reactive deprotonated form is of tautomeric type, forming 9-anthranolate ion. This ion can react not only as a nucleophile but also as a diene in Diels–Alder addition with reactive dienophiles. Indeed, asymmetric [4 + 2] cycloadditions of **2** to *N*-substituted maleimides catalyzed by chiral Brönsted bases have been reported.[8–10] However, with $\alpha,\beta$-unsaturated esters, ketones and nitro compounds conjugate addition of **2** is the preferred mode of reaction.[11,12] Asymmetric additions of **2** to $\alpha,\beta$-unsaturated aldehydes catalyzed by a derivative of prolinol[13] and to enones using a thiourea derivative of 9-amino-9-deoxyepiquinine as a catalyst[14] have been recently disclosed.

We anticipated that addition of **2** to **1** could be achieved in enantioselective fashion to give product **3** as a key intermediate for the synthesis of the title compound **5**. As a catalyst of the addition L-proline or its derivatives could be used on the basis of literature data discussed previously. Further steps of synthesis are shown in Scheme 2 and include diastereoselective reduction of the carbonyl groups to give diol **4** and selective dehydration to produce anthracene substituted product **5**.

## EXPERIMENTAL SECTION

$^1$H nuclear magnetic resonance (NMR) and $^{13}$C NMR spectra were recorded with Bruker Avance II 400 and Varian Oxford 300 spectrometers. Chemical shift values are given in parts per million (ppm) relative to tetramethylsilane (TMS). Column chromatography was performed using Fluka 60 (70–230 mesh) silica gel, and thin layer chromatography was carried out with Fluka silica gel precoated plates. Fourier transform infrared spectroscopy spectra were recorded with a Bruker IFS 66v/S spectrometer. High-resolution mass spectrometry (HR-MS) spectra were obtained with a Bruker 320 MS spectrometer. High-performance liquid chromatography (HPLC) analyses were carried out on a Chiralpak-IA column by using mobile phase and flow rate as indicated. UV and circular dichroism (CD) spectra were recorded with a Jasco J-810 spectropolarimeter. Melting points were determined on a Büchi Melting Point B-545 apparatus and are uncorrected. All reagents were used as purchased from commercial suppliers. All solvents were provided by a local supplier and were purified by conventional methods prior to use. Commercial diphenyl-L-prolinol and its *O*-TMS derivative were used as received. Methyl L-prolinate was obtained as hydrochloride salt from which the free base was extracted with $CH_2Cl_2$–saturated $NaHCO_3$ solution prior to use.

### *Computational Methods*

Starting geometries of dienes **3** and **6** with assumed absolute configurations were obtained by conformational search with the use of a CONFLEX software and preoptimization of all conformers at the B3LYP/6-31G(d) level. This allowed identification of the minimum energy structures, which were further reoptimized in acetonitrile or methanol solutions, using the polarizable continuum model (integral equation formalism polarizable continuum model (IEFPCM))[15] with the use of the newly developed M06-2X[16] hybrid functionals, in conjunction with 6-311++G(2d,2p) basis set. The structures thus obtained were the real minimum energy conformers (no imaginary frequencies have been found). The total and free energy values were used to obtain the Boltzmann population of conformers at 298.15 K. For density functional theory (DFT) calculations, only the results for conformers that differ from the most stable one by less than 2 kcal mol$^{-1}$ were taken into account, following a generally accepted protocol.[17]

The calculations of optical rotations were carried out for all stable conformers of **3** at $[\alpha]_D$ wavelength (589 nm), in the solvent, using the B3LYP/6-311++G(2d,2p) method. London orbitals (which ensure the origin independency of the results) have been used.[18]

For all investigated compounds, electronic circular dichroism (ECD) spectra were measured in acetonitrile solution and calculated at the IEFPCM/TDDFT/6-311++G(2d,2p) level for all stable geometries optimized at the IEFPCM/M06-2X/6-311++G(2d,2p) level, according to the procedure previously described.[19] We employed five different hybrid functionals to calculate ECD spectra: M06-2X,[20] PBE0,[21] B2LYP,[22] LC-wPBE,[23] and CAM-B3LYP.[24]

Contract grant sponsor: National Centre of Science (Poland), program OPUS 2.
*Correspondence to: Jacek Gawronski, Department of Chemistry, Adam Mickiewicz University, 60780 Poznan, Poland.
E-mail: gawronsk@amu.edu.pl
Received for publication 12 April 2012; Accepted 11 May 2012
DOI: 10.1002/chir.22079
Published online in Wiley Online Library (wileyonlinelibrary.com).

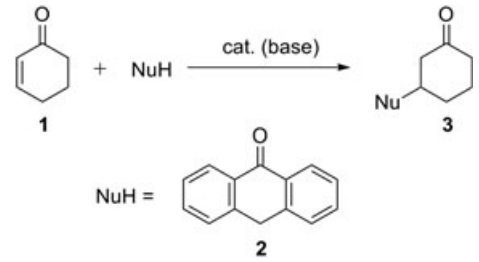


**Scheme 1.** Nucleophilic additions to 2-cyclohexenone.

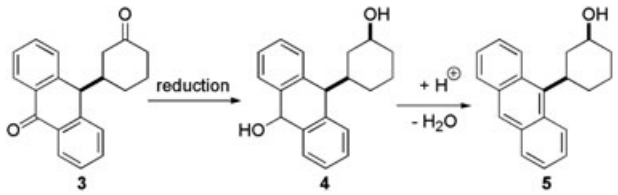


**Scheme 2.** Route to cis-3-(9-anthryl)cyclohexanol.

Rotatory strengths were calculated using both length and velocity representations. In the present study, the differences between the length and velocity calculated values of rotatory strengths were quite small, and for this reason, only the velocity representations were further used. The ECD spectra were simulated by overlapping Gaussian functions[25] for each transition, according to the procedure previously described.[26]

All calculations were performed with the use of CAChe-WS Pro, Gaussian 09, and Turbomole 6.0 packages.[27–29]

### *General Procedure for Addition of 2 to 1*

*Analytical procedure*: **2**, **1**, and the catalyst in appropriate amounts (Tables 1–3) were dissolved in a solvent (1 ml) in a 4-ml reaction vial. The mixture was stirred in the darkness for 66 h, then quenched with 1 M HCl solution, extracted with $CH_2Cl_2$ (3 × 10 ml), dried over $MgSO_4$, the solution filtered and evaporated. The product (**3**), a white solid, was isolated by centrifugal chromatography (eluent: hexane/EtOAc, 9:1); $^1$H NMR (400 MHz, $CDCl_3$): δ 0.99–1.16 (m, 1H), 1.34–1.54 (m, 1H), 1.70–1.75 (m, 1H), 1.83–2.08 (m, 3H), 2.16–2.35 (m, 3H), 4.22 (d, $J$ = 3.1 Hz, 1H), 7.39 (d, $J$ = 7.6 Hz, 1H), 7.49 (m, 3H), 7.61 (d, $J$ = 7.3 Hz, 2H), 8.28 (m, 2H); $^{13}$C NMR (100 MHz, $CDCl_3$): δ 24.8, 27.5, 40.9, 45.3, 48.4, 48.6, 127.1, 127.2, 127.4, 127.6, 128.5, 128.7, 132.5, 132.6, 133.3, 133.4, 141.7, 142.3, 185.1, 210.5; HR-MS: $m/z$ calcd for $C_{20}H_{18}NaO_2$ ($[M + Na]^+$): 313.1204, found: 313.1238, calcd for $C_{40}H_{36}NaO_4$ ($[2M + Na]^+$): 603.2511, found: 603.2510.

*Large-scale procedure*: **2** (1165.4 mg, 6.0 mmol), **1** (1.16 ml, 12.0 mmol), and **Cat1** (69.1 mg, 0.6 mmol) were dissolved in MeCN (20 ml) and stirred in dark for 66 h, then quenched with 1 M HCl solution, extracted with $CH_2Cl_2$ (3 × 30 ml), dried over $MgSO_4$, filtered, and evaporated. The residue was dissolved in $CH_2Cl_2$ and filtered through a short silica gel column to separate the substrates from the products. The colorless oily mixture of **3** and traces of 10,10′-dihydrobianthrone as a side product was triturated dropwise with diethyl ether to afford **3** as a white solid (1219 mg, yield 70%, $[\alpha]_D^{25} = -5.7°$ ($c$ = 0.71, methanol), ee 80%, mp 107–109 °C).

The racemate of **3** was prepared with the same procedure using 194.2 mg (1.0 mmol) of **2**, 193.6 µl (2.0 mmol) of **1**, 13.9 mg (0.1 mmol) of pyridinium acetate as catalyst, and 4 ml of $CH_2Cl_2$ as solvent. Yield of *rac*-**3** 220.7 mg (76%), mp 135–136 °C.

**TABLE 1. Results of screening catalyst efficiency**[a]

| Entry | Catalyst | Yield of **3** (%) | Ee[b] (%) |
|---|---|---|---|
| 1 | **Cat1** | **32** | **82** |
| 2 | **Cat2** | 39 | 0 |
| 3 | **Cat3** | 0 | – |
| 4 | **Cat4** | 0 | – |
| 5 | **Cat5** | 15 | 5 |

Entry in bold shows optimum result.
[a]Conditions: **2**:**1** = 0.35:0.30 mmol, catalyst 20 mol%, $CH_2Cl_2$ (1 ml), 66 h, room temperture.
[b]Determined by chiral high-performance liquid chromatography analysis after purification.

**TABLE 2. Results of solvent screening with *Cat1* as a catalyst**[a]

| Entry | Solvent | Yield of **3** (%) | Ee (%) |
|---|---|---|---|
| 1 | $CH_2Cl_2$ | 32 | 82 |
| 2 | PhMe | 7 | 39 |
| 3 | THF | 9 | 47 |
| 4 | $Et_2O$ | 17 | 55 |
| 5 | EtOAc | 3 | 50 |
| 6 | $Me_2CO$ | 16 | 52 |
| **7** | **MeCN** | **43** | **86** |
| 8 | DMF | 73 | 0 |
| 9 | DMSO | 46 | 0 |
| 10 | MeOH | 9 | 0 |

Entry in bold shows optimum result.
[a]For experimental details, see Table 1.

**TABLE 3. Results of catalyst amount screening**[a]

| Entry | Ratio of **2**:**1** | Cat1 (mol%) | Yield of **3** (%) | Ee[b] (%) |
|---|---|---|---|---|
| 1 | 1:1.2 | 5 | 19 | 85 |
| 2 | 1:1.2 | 10 | 39 | 86 |
| 3 | 1:1.2 | 20 | 36 | 86 |
| 4 | 1:2 | 5 | 62 | 85 |
| **5** | **1:2** | **10** | **76** | **87** |
| 6 | 1:2 | 20 | 69 | 87 |

Entry in bold shows optimum result.
[a]Conditions: **1** = 0.3 mmol, MeCN (1 ml), 66 h, room temperture.
[b]Determined by chiral high-performance liquid chromatography after purification.

### *Diastereoselective Reduction of Michael Adduct 3 with $NaBH_4$ to 4*

Michael adduct **3** (20.0 mg, 67.9 µmol, 80% ee) was dissolved in MeOH (1.5 ml) and cooled to 0 °C in an ice bath. Then, $NaBH_4$ (10.3 mg, 271.6 µmol, 4 eq) was added. The reaction mixture was stirred for 1 h at room temperature, followed by quenching with water. The mixture was transferred to a separatory funnel and extracted with $CH_2Cl_2$ (3 × 10 ml). The combined organic extracts were dried over $MgSO_4$, filtered, and evaporated. Purification by column chromatography (eluent: hexane/EtOAc, 4:1) furnished 16.0 mg (79%) of a mixture of diastereomers of **4** (dr 12:1).

### *Diastereoselective Reduction of Michael Adduct 3 with $LiAlH_4$ to 4*

The reaction was carried out under argon atmosphere. Michael adduct **3** (20.0 mg, 67.9 µmol, 80% ee) was dissolved in dry tetrahydrofuran (THF) (1.5 ml) and the solution cooled to −78 °C (2-propanol-dry ice bath). The solution was added dropwise to a suspension of $LiAlH_4$ cooled to −78 °C (10.3 mg, 271.6 µmol, 4 eq) in dry THF (2 ml). The reaction mixture was stirred 1 h at room temperature, followed by quenching with ethyl acetate. The mixture was filtered through celite using ethyl acetate and evaporated. The residue was dissolved in $CH_2Cl_2$ (10 ml), transferred to a separatory funnel, and washed with brine (10 ml). The organic layer was dried over $MgSO_4$, filtered, and evaporated to afford crude product in quantitive yield. Purification (silica gel column, eluent: hexane/EtOAc, 4:1) furnished **4** (19.9 mg, 98%) as a mixture of diastereoisomers (dr 12:1; equatorial : axial hydroxy group).

Large-scale procedure was similar to that previously described, using **3** (200 mg, ee 80%) dissolved in THF (15 ml) and $LiAlH_4$ (103 mg) in THF (20 ml). The product (201 mg) was a mixture of diastereoisomers. Crystallization afforded enantiomer **4**, mp 127–130 °C (ee >99%, HPLC); $^1$H NMR (400 MHz, $CDCl_3$): δ 0.80–1.10 (m, 3H), 1.35 (bs, 1H), 1.43–1.52 (m, 2H), 1.65–1.74 (m, 1H), 1.77–1.88 (m, 2H), 2.15 (d, $J$ = 10.6 Hz, 1H), 3.29–3.44 (m, 1H), 3.72 (d, $J$ = 7.5 Hz, 1H), 5.67 (d, $J$ = 10.5 Hz, 1H), 7.22–7.36 (m, 6H), 7.79 (d, $J$ = 7.6 Hz, 2H); $^{13}$C NMR (100 MHz, $CDCl_3$): δ 23.7, 30.0, 35.3, 40.6, 42.8, 52.8, 67.8, 70.8, 124.3, 126.6, 126.8, 128.7, 137.0, 140.3; HR-MS: $m/z$ calcd for $C_{20}H_{22}NaO_2$ ($[M+Na]^+$): 317.1517, found: 317.1474.

### *Dehydration of 4 to 5 with Dowex® 50W*

Dowex® 50 W (30 mg) was added to a solution of **4** (20 mg, 67.9 μmol, ee > 99%) cooled to 0 °C in $CH_2Cl_2$ (1.5 ml), and the mixture was stirred for 3 days at room temperature. After filtration, the crude product was purified by column chromatography (eluent: hexane/EtOAc, 15:1) to afford **5** as a yellowish solid (15.8 mg, 84%), mp 121–123 °C; $^1$H NMR (400 MHz, $CDCl_3$): δ 1.59–1.77 (m, 2H), 1.82–1.94 (m, 1H), 2.01–2.13 (m, 1H), 2.16–2.31 (m, 2H), 2.39–2.50 (m, 1H), 2.53 (q, $J$ = 12.8 Hz, 1H), 3.87–4.03 (m, 1H), 4.18 (tt, $J$ = 12.8, 3.4 Hz, 1H), 7.39–7.53 (m, 4H), 8.00 (d, $J$ = 8.9 Hz, 2H), 8.35 (s, 1H), 8.60 (bs, 1H); $^{13}$C NMR (100 MHz, $CDCl_3$): δ 25.3, 30.6, 35.6, 37.9, 41.1, 71.8, 123.5, 124.6, 125.8, 126.3, 126.9, 129.6, 129.7, 137.0; HR-MS: $m/z$ calcd for $C_{21}H_{24}KNaO_2$ ($[M+K+Na+MeOH]^+$): 370.1311, found: 370.0916.

Large-scale procedure was the same as described previously using 170 mg of **4** (577 μmol, ee >99%), 255 mg of Dowex® 50W resin, and 13 ml of $CH_2Cl_2$ as a solvent. Yield 137.7 mg of **5** (86%).

(1*S*,3*R*)-3-(9-*Anthryl*)*cyclohexyl benzoate* (**6**): (1*S*,3*R*)-3-(9-Anthryl) cyclohexanol (**5**) (20.0 mg, 72.4 μmol) was dissolved in pyridine (1 ml). Then, benzoyl chloride (25.1 μl) was added, and the reaction mixture was gently refluxed for 2 h. Saturated $NaHCO_3$ (5 ml) solution was added dropwise, and the resulted mixture was transferred to a separatory funnel. After extraction of the aqueous phase with $CH_2Cl_2$ (3 × 10 ml), the combined organic phases were dried over $MgSO_4$, filtered, and evaporated. Crude product was purified by column chromatography (eluent: hexane/EtOAc, 30:1) furnishing **6** (18.6 mg, 68%) as a colorless solid, $^1$H NMR (400 MHz, $CDCl_3$): δ 1.77–1.89 (m, 2H), 1.96 (m, 1H), 2.07–2.21 (m, 1H), 2.31–2.46 (m, 2H), 2.45–2.63 (m, 1H), 2.77 (q, $J$ = 12.6 Hz, 1H), 4.24–4.39 (m, 1H), 5.24–5.41 (m, 1H) 7.38–7.58 (m, 7H), 8.00 (d, $J$ = 8.3 Hz, 2H), 8.04 (d, $J$ = 8.3 Hz, 2H), 8.35 (s, 1H), 8.39 (bs, 1H) 8.64 (bs, 1H); $^{13}$C NMR (100 MHz, $CDCl_3$): δ 25.2, 30.6, 32.0, 37.1, 38.0, 74.3, 123.6, 124.4, 126.0, 127.0, 128.3, 129.6, 129.7, 130.7, 132.9, 136.5, 166.0.

## RESULTS AND DISCUSSION

### *Synthesis*

L-Proline and its derivatives were screened as catalysts for enantioselective Michael addition of **2** to **1** (Fig. 1).

Standard reaction carried out in dichloromethane solution at room temperature (Table 1) was successful with L-proline (**Cat1**) as organocatalyst to give **3** in moderate yield and good ee Methyl L-prolinate (**Cat2**) gave racemic addition product **3**. Neither hydroxy derivative of L-proline (**Cat3**) nor diphenyl-L-prolinol (**Cat4**) was successful as catalysts.

Hayashi's catalyst (**Cat5**) gave product **3** with poor yield and low ee This seemed surprising because similar addition

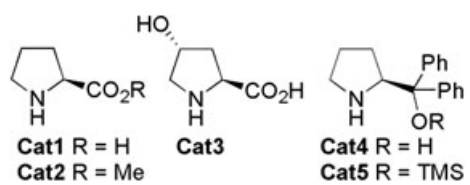


**Fig. 1.** Catalysts used in asymmetric Michael-type addition of **2** to **1**.

reactions of **2** to α,β-unsaturated aldehydes as acceptors were reported to give excellent results under optimized conditions.[13]

It is of importance to note that the aforementioned addition reactions were heterogeneous because of poor solubility of **2** in the reaction medium. Except in $CH_2Cl_2$, both yield and enantioselectivity of the reaction in solvents of low polarity were low (Table 2, entries 2–6).

Dimethyl sulfoxide is often used as a solvent when L-proline is used as a catalyst. In the experiment carried out, only racemic **3** was formed in moderate yield. The same applies to other polar solvents, DMF and MeOH (entries 8–10, Table 2).

The use of MeCN (entry 7, Table 2) increased both the yield and enantiomeric excess of **3** compared with those obtained with $CH_2Cl_2$ as a solvent. Therefore, MeCN was chosen as a solvent for further reactions. There was still a problem of unsatisfactory yield of the reaction. Therefore, the effect of ratio of the two reactants, **2** and **1**, on the yield of the reaction was examined next. Increase of the ratio of **2**:**1** from 1:1 to 1:5 resulted in gradual increase of the yield of **3** from 35% to 80%, whereas ee of the product remained essentially unchanged (86–87%). Further increase of the excess of **1** had no effect on the yield of **3**. Because of practical reasons (product separation), the 1:2 ratio of **2**:**1** was chosen, as a compromise between the optimum conditions and the cost/operational simplicity.

Organocatalysis often requires considerable amount of the catalyst to achieve good enantioselectivity and yield of the reaction. Although in the preliminary experiments we used 20 mol% of the catalyst, we then determined the optimum molar amount of the catalyst. It was found that for the two ratios of substrates **2**:**1** (1:1.2 and 1:2), the ee of product **3** did not differ much, the yield depended on the amount of L-proline used and was the highest with 10 mol% of the catalyst (in relation to anthrone **2**, see Table 3).

As the final step, we checked the effect of temperature on the yield and ee of the addition product **3**. We found that lowering reaction temperature shows little effect on the ee of **3**, whereas it has an adverse effect on the reaction yield. Thus, room temperature was found the most suitable for this reaction.

The highest obtained ee of the addition product **3** (87%) compares favorably with the ee of the product obtained with the aid of a much more expensive cinchona alkaloid–thiourea organocatalyst (78%).[14]

Having determined the optimum conditions for the synthesis of **3** (2 eq. of **1**, 1 eq. of **2**, 0.1 eq. of L-proline, solvent MeCN, room temperature), we attempted to increase the initial enantiomeric purity of product **3** by crystallization. Crystallization from toluene–hexane led, however, to a decrease of ee of **3** in the crystals, whereas the filtrate contained **3** of higher ee (Fig. 2). Such a behavior is not favorable for enantiomer separation by crystallization and is typical for molecules crystallizing preferentially as racemic compounds. This is confirmed by comparison of the melting points of *rac*-**3** (135–136 °C) and enantiomerically pure **3** (107–109 °C). For substances crystallizing as racemic compounds, the difference of melting points is typically 25–30 °C.

Consequently, we decided to reduce first the carbonyl functions of **3** in diastereoselective manner. The best results were obtained with $LiAlH_4$ (4 eq.) in THF solution. The reduction of **3** (ee 80%) proceeded in quantitive yield at the temperature of

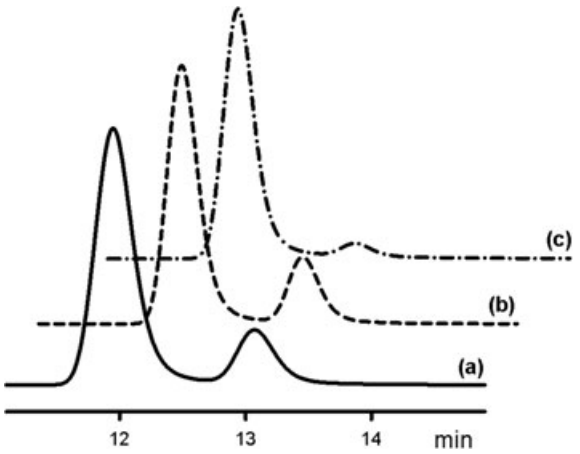


**Fig. 2.** High-performance liquid chromatography traces showing the results of crystallization of **3**: (a) initial sample of **3**, ee 62%; (b) crystals of **3**, ee 56%; (c) filtrate containing **3**, ee 83%.

dry ice–2-propanol bath. While diastereomeric ratio of the products was at the level of 12:1 (*cis*:*trans*), further experiments have shown that just one crystallization from ethyl acetate–*n*-hexane furnished **4** as a single stereoisomer, yield 64% (Fig. 3). Reduction of **3** with $NaBH_4$ in methanol at 0 °C proceeded with a similar diastereoselectivity (12:1); however, the yield of crude reduction products was lower (79%).

To finalize the synthesis, **4** was chemoselectively dehydrated under acidic conditions to form the anthracene substituent in **5**. Out of several acids tried, Dowex® 50W resin provided a very convenient way to obtain the final product in 84% yield, although the reaction time was long (3 days). Dehydration with methanesulfonic acid proceeded considerably faster even at 0 °C; however, the yield of isolated **5** was lower (47%) because of contamination with side products.

Interestingly, the analysis of the $^1$H NMR spectrum of **5** showed that both groups, hydroxy and anthryl, were equatorial. The signal of $H_a$ at 4.18 ppm was split into a triplet of triplets ($J$ = 12.8 Hz and 3.4 Hz). The value $J$ = 12.8 Hz is typical for vicinal diaxial proton arrangements, whereas $J$ = 3.4 Hz is typical for vicinal axial-equatorial proton couplings. This means that there are two vicinal axial and two vicinal equatorial protons that are coupled to axial proton $H_a$, whereas the anthryl group is equatorial (Fig. 4).

A similar situation is found for proton $H_b$. The signal at 2.53 ppm is split into a quartet with a coupling constant $J$ = 12.8 Hz. This is a typical value for both geminal and vicinal diaxial proton coupling constants. Therefore, the hydroxy group is equatorial, whereas $H_b$ is axial and coupled to one geminal and two vicinal axial protons.

### *Absolute Configuration of the Michael Adduct 3*

Whereas the relative configuration of substituents in **5** was determined by $^1$H NMR spectroscopy, the absolute configuration at the stereogenic C3 atom was subsequently established using a method of comparing experimental and calculated optical rotation data and CD spectra of the Michael adduct **3**.

Initially, low energy structures of **3**, with assumed *R* absolute configuration at the stereogenic center, were calculated using molecular mechanics method followed by preoptimization at the B3LYP/6-31G(d) level. This furnished six stable conformers, three of which with the equatorial anthrone substituent and the other three with the axial substituent. The structures of the conformers were then reoptimized at the M06-2X/6-311++G(2d,2p) level in conjunction with the polarizable continuum model simulating acetonitrile or methanol solution. Conformers with axial anthrone substituent were found to be of much higher energy (over 3 kcal mol$^{-1}$), and their population in the equilibrium was negligible in comparison with the equatorial ones. The diequatorial conformers of **3** are shown in Figure 5, and their relative energies and values of dihedral angle $\omega$ = H-C3-C(Ar)-H that characterize the conformation are collected in Table 4. It is important to note that the conformers differ with regard to the torsion angle $\omega$, involving two secondary carbon atoms. It can be either *gauche*

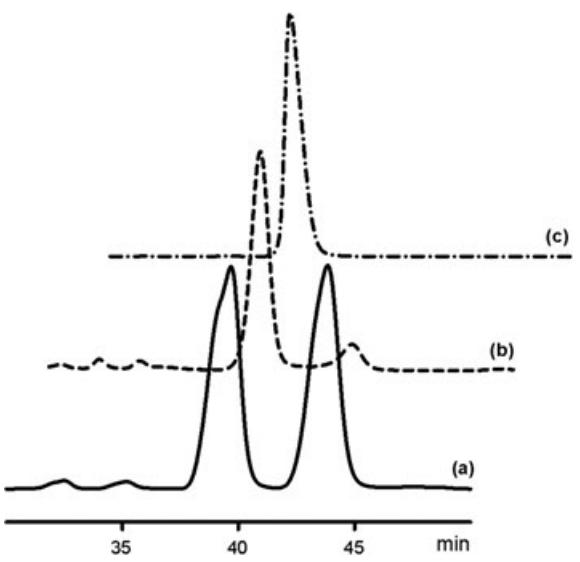


**Fig. 3.** High-performance liquid chromatography traces showing changes of dr and ee of product **4** because of crystallization: (a) *rac*-**4**; (b) **4** prior to crystallization, ee 80%; (c) **4** after one crystallization, ee >99%.

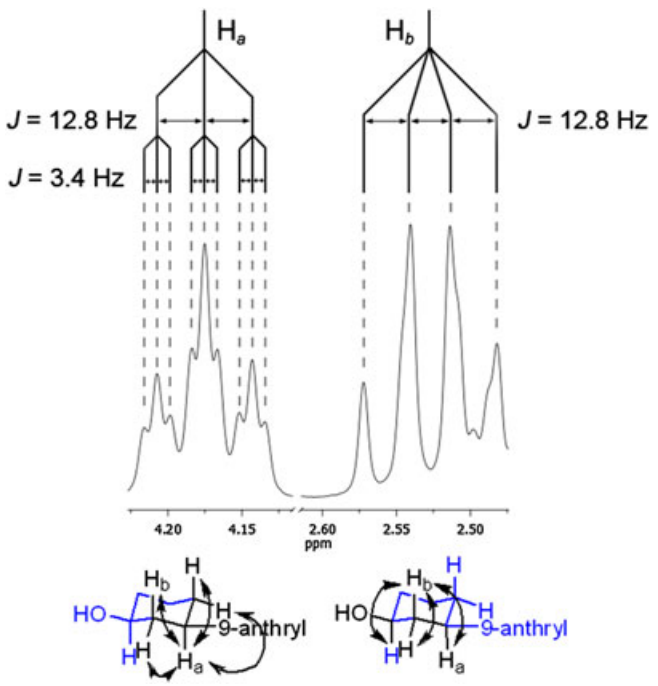


**Fig. 4.** Coupling pattern of protons $H_a$ and $H_b$ in the $^1$H nuclear magnetic resonance spectrum of **5**.

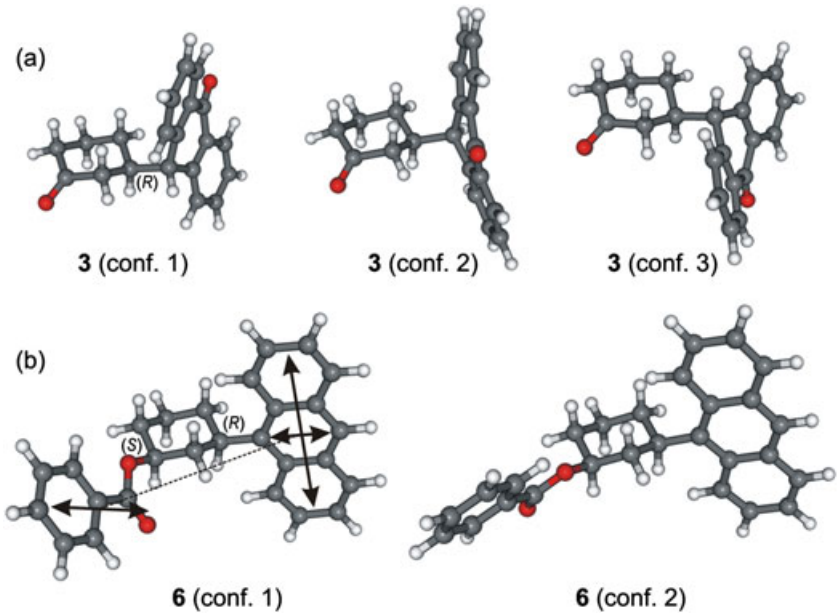


**Fig. 5.** Structures of individual conformers of (**a**) (*R*)-**3** and (**b**) benzoate (1*S*,3*R*)-**6** calculated at the IEFPCM/M06-2X/6-311++G(2d,2p) level.

**TABLE 4. Total energies (in Hartree), relative energies (*E*, *G* in kcal mol$^{-1}$), percentage populations, and values of torsion angles $\omega$ (in degrees) calculated at the IEFPCM/M06-2X/6-311++G(2d,2p) level for individual conformers of 3 and 6**

| Conformer | Energy | *E* | Population | *G* | Population | $\omega$[a] |
|---|---|---|---|---|---|---|
| **3** (conf. 1) | −923.3561525 | 0.00 | 51 | 0.00 | 53 | 63.8 |
| **3** (conf. 2) | −923.3560365 | 0.07 | 46 | 0.19 | 39 | −65.3 |
| **3** (conf. 3) | −923.3534997 | 1.66 | 3 | 1.14 | 8 | 176.9 |
| **6** (conf. 1) | −1193.685516 | 0.00 | 58 | 0.25 | 40 | — |
| **6** (conf. 2) | −1193.685227 | 0.18 | 42 | 0.00 | 60 | — |

[a]$\omega$ = H–C3–C(Ar)–H in **3**.

(+ or −) or *anti*, whereas the cyclohexanone ring remains in a chair form.

The measured optical rotation of **3** was $[\alpha]_D^{25} = -5.7°$ ($c = 0.71$, methanol) for a sample of ee 80%. When corrected to 100% ee, this corresponds to the specific rotation −7.2° and is in good accordance with the value calculated at the IEFPCM/B3LYP/6-311++G(2d,2p) level for the *R* enantiomer (−9.4°), using the conformer population calculated at the IEFPCM/M06-2X/6-311++G(2d,2p) level.

The five density functionals, which have been tested, i.e., M06-2X, PBE0, B2LYP, LC-wPBE, and CAM-B3LYP, differ in the amount of Hartree-Fock XC and the philosophy of their construction.[30] The best agreement with the experiment was found when either M06-2X or CAM-B3LYP functional was employed.[31] The *G* based Boltzmann averaged CD spectra of (*R*)-**3**, calculated at the IEFPCM/M06-2X/6-311++G(2d,2p) level, as well as the experimentally measured spectrum, are shown in Figure 6. The match of the signs and magnitudes of the Cotton effects is barely acceptable, even if the differences in the wavelengths (energies) of transitions are neglected. It is worth to note that other functionals gave no better results.

A confirmation of the absolute configuration of target molecule **5** was obtained from the CD spectrum of its benzoate derivative **6**, using the CD exciton chirality method.[32] Introduction of the benzoate chromophore to **5** makes the molecule bichromophoric. The experimental and calculated ECD spectra of **6** are shown in Figure 6.

The presence of a negative exciton couplet in the range of 265–215 nm is due to the negative sign of the dihedral angle between the electric dipole transition moment of the benzoate chromophore and the electric transition moment along the longitudinal axis of the anthracene chromophore (Fig. 5b). Additionaly, there is also a second, positive exciton couplet in the range 210–185 nm, which refers to the positive sign of the dihedral angle between the transition moment of the benzoate, as in the first couplet, and the electric dipole transition moment polarized along shorter axis of the anthracene chromophore. These two facts establish the 1*S*,3*R* absolute configuration of the two chiral carbon atoms in molecule **6** and hence also in target molecule **5**.

The predictions based on empirical exciton chirality rule were further confirmed by calculation of ECD spectrum of **6** with the use of TDDFT methods. In this case, we observed almost perfect agreement between the calculation and the experiment. Because the observed Cotton effects of **6** are generated by electronic transitions within the π-electron systems, the calculated CD spectrum of **6** is more reliable than that of **3**. All density functionals tested gave consistent

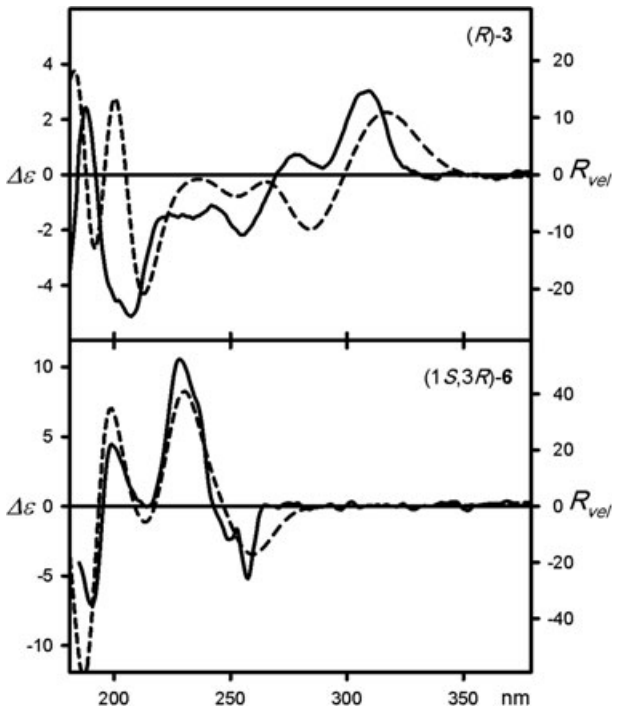


**Fig. 6.** Electronic circular dichroism spectra of (upper panel) (*R*)-**3** and (lower panel) (1*S*,3*R*)-**6**, experimental measured in acetonitrile solution (solid lines) and *G*-based Boltzmann averaged calculated at the IEFPCM/M06-2X/6-311++G(2d,2p) level (dashed lines). All calculated spectra were wavelength corrected to match the experimental UV maxima.

results; however, we observed the best match when M06-2X hybrid was employed.

In conclusion, (*R*)-**3** enantiomer was found to be the major product of the addition of anthrone to 2-cyclohexenone, with L-proline as the catalyst. The described procedure represents a convenient and way to obtain enatiomerically pure *cis*-3-(9-anthryl)cyclohexanol.

## ACKNOWLEDGMENT

All calculations were performed at Poznań Supercomputing Center, Poland.

## LITERATURE CITED

1. Sasai H, Arai T, Satow Y, Houk KN, Shibasaki M. The first heterobimetallic multifunctional asymmetric catalyst. J Am Chem Soc 1995;117:6194–6198.
2. Jansen JFGA, Feringa BL. Enantioselective conjugate addition of Grignard reagents to enones catalyzed by chiral zinc(II) complexes. J Org Chem 1990;55:4168–4175.
3. Feringa BL. Phosphoramidites: marvellous ligands in catalytic asymmetric conjugate addition. Acc Chem Res 2000;33:346–353.
4. Zweifel T, Hollmann D, Prüger B, Nielsen M, Jørgensen KA. Combined organo- and gold-catalyzed enantioselective synthesis of bicyclic enones. Tetrahedron: Asymmetry 2010;21:1624–1629.
5. Hiemstra H, Wynberg H. Addition of aromatic thiols to conjugated cycloalkenones, catalyzed by chiral β-hydroxy amines. A mechanistic study of homogeneous catalytic asymmetric synthesis. J Am Chem Soc 1981; 103:417–430.
6. Rana NK, Selvakumar S, Singh VK. Highly enantioselective organocatalytic sulfa-Michael addition to α,β-unsaturated ketones. J Org Chem 2010;75:2089–2091.
7. Zhou Y, Li X, Li W, Wu C, Liang X, Ye J. Asymmetric organocatalytic Michael addition of α,β-unsaturated ketone with 1,2,4-triazole. Synlett 2010;15:2357–2360.
8. Tokioka K, Masuda S, Fujii T, Hata Y, Yamamoto Y. Asymmetric cycloaddition of anthrone with N-substituted maleimides with $C_2$-chiral pyrrolidines. Tetrahedron: Asymmetry 1997;8:101–107.
9. Shen J, Nguyen TT, Goh Y-P, Ye W, Fu X, Xu J, Tan C-H. Chiral bicyclic guanidine-catalyzed enantioselective reactions of anthrones. J Am Chem Soc 2006;128:13692–13693.
10. Akalay D, Dürner G, Göbel MW. A first case of asymmetric catalysis induced by metal-free bisoxazolines. Eur J Org Chem 2008;2365–2368.
11. Baik W, Yoon CH, Lee KC, Lee HJ, Koo S, Kim J, Yoon H, Kim H. Chemoselective reactions of anthrone with α,β-unsaturated ketones. J Chem Res (S) 1998;358–359. Baik W, Yoon CH, Koo S, Kim H, Kim J, Hong S. Lewis acid-catalyzed reactions of anthrone: preference for cycloaddition reaction over conjugate addition depending on the functionality of α,β-unsaturated carbonyl compounds. Bull Korean Chem Soc 2004;25:491–500.
12. Shi M, Lei ZY, Zhao MX, Shi JW. A highly efficient asymmetric Michael addition of anthrone to nitroalkenes with cinchona organocatalysts. Tetrahedron Lett 2007;48:5743–5746.
13. Alba A-N, Bravo N, Moyano A, Rios R. Enantioselective addition of anthrones to α,β-unsaturated aldehydes. Tetrahedron Lett 2009;50:3067–3069.
14. Wu C, Li W, Yang J, Liang X, Ye J. Asymmetric organocatalytic Michael addition of anthrone to enone. Org Biomol Chem 2010;8:3244–3250.
15. Scalmani G, Frisch MJ. Continuous surface charge polarizable continuum models of solvation. I. General formalism. J Chem Phys 2010;132:114110
16. Zhao Y, Truhlar DG. The M06 suite of density functionals for main group thermochemistry, thermochemical kinetics, noncovalent interactions, excited states, and transition elements: two new functionals and systematic testing of four M06-class functionals and 12 other functionals. Theor Chem Acc 2008;120:215–241.
17. Stephens PJ, McCann DM, Devlin FJ, Cheeseman JR, Frisch MJ. Determination of the absolute configuration of [32](1,4)barrelenophanedicarbonitrile using concerted time-dependent density functional theory calculations of optical rotation and electronic circular dichroism. J Am Chem Soc 2004;126:7514–7521.
18. Pecul M, Ruud K, Helgaker T. Density functional theory calculation of electronic circular dichroism using London orbitals. Chem Phys Lett 2004;388:110–119.
19. Kwit M, Gawronski J, Boyd DR, Sharma ND, Kaik M. Circular dichroism, optical rotation and absolute configuration of 2-cyclohexenone-*cis*-diol type phenol metabolites: redefining the role of substituents and 2-cyclohexenone conformation in electronic circular dichroism spectra. Org Biomol Chem 2010;8:5635–5645.
20. Jacquemin D, Perpète EA, Ciofini I, Adamo C, Valero R, Zhao Y, Truhlar DG. On the performances of the M06 family of density functionals for electronic excitation energies. J Chem Theor 2010;6:2071–2085.
21. Adamo C, Barone V. Toward reliable density functional methods without adjustable parameters: the PBE0 model. J Chem Phys 1999;110:6158–6169.
22. Goerigk L, Grimme S. Calculation of electronic circular dichroism spectra with time-dependent double-hybrid density functional theory. J Phys Chem A 2009;113:767–776.
23. Tawada Y, Tsuneda T, Yanagisawa S, Yanai T, Hirao K. A long-range-corrected time-dependent density functional theory. J Chem Phys 2004;120:8425.
24. Yanai T, Tew D, Handy N. A new hybrid exchange-correlation functional using the Coulomb-attenuating method (CAM-B3LYP). Chem Phys Lett 2004;393:51–57.
25. Harada N, Stephens P. ECD cotton effect approximated by the Gaussian curve and other methods. Chirality 2010;22:229–233.
26. Gawronski J, Kwit M, Boyd DR, Sharma ND, Malone JF, Drake AF. Absolute configuration, conformation and circular dichroism of monocyclic arene dihydrodiol metabolites: it is all due to the heteroatom substituents. J Am Chem Soc 2005;127:4308–4319.
27. CAChe WS Pro 4.5, Fujitsu Ltd.
28. Robb MA, Cheeseman JR, Montgomery JA, Vreven Jr T, Kudin KN, Burant JC, Millam JM, Iyengar SS, Tomasi J, Barone V, Mennucci B, Cossi M, Scalmani G, Rega N, Petersson GA, Nakatsuji H, Hada M, Ehara M, Toyota K, Fukuda R, Hasegawa J, Ishida M, Nakajima T, Honda Y, Kitao O, Nakai H, Klene M, Li X, Knox JE, Hratchian HP, Cross JB, Bakken V, Adamo C, Jaramillo J, Gomperts R, Stratmann RE, Yazyev O, Austin AJ, Cammi R, Pomelli C, Ochterski JW, Ayala PY, Morokuma K, Voth GA, Salvador P, Dannenberg JJ, Zakrzewski VG, Dapprich S, Daniels AD, Strain MC, Farkas O, Malick DK, Rabuck AD, Raghavachari K, Foresman JB, Ortiz JV, Cui Q, Baboul AG, Clifford S, Cioslowski J, Stefanov BB, Liu G, Liashenko A, Piskorz P, Komaromi I, Martin RL, Fox DJ, Keith T, Al-Laham MA, Peng CY, Nanayakkara A, Challacombe M, Gill PMW, Johnson B, Chen W, Wong MW, Gonzalez C, Pople JA. Gaussian 03 (Revision D.0). Gaussian, Inc.: Wallingford CT, 2004.

29. Ahlrichs R, Bär M, Häser M, Horn H, Kölmel C. Electronic structure calculations on workstation computers: the program system TURBOMOLE. Chem Phys Lett 1989;162: 165–169, for more information see: http://www.cosmologic.de.
30. Cohen AJ, Mori-Sánchez P, Yang W. Challenges for Density Functional Theory. Chem Rev 2012;112:289–320.
31. These studies are a part of the project focused on improving the performance of modern theoretical methods for the prediction of chiroptical properties of organic compounds representing so called "difficult" cases.
32. Harada N, Nakanishi K. Circular dichroic spectroscopy – exciton coupling in organic stereochemistry. University Science Books: Mill Valley, CA, 1983.